International Journal of the Physical Sciences Vol. 5 (9), pp. 1450-1464, 18 August, 2010
Available online at http://www.academicjournals.org/IJPS
ISSN 1992 - 1950 © 2010 Academic Journals

Full Length Research Paper

Theoretical investigation of dielectric effects on nanostructure of β - amyloid peptide

L. Pishkar[1], M. Monajjemi[2], A.R. Ilkhani[3] and F. Mollaamin[2*]

[1]Ph.D Student, Science and Research Branch, Islamic Azad University, Tehran, Iran.
[2]Department of Chemistry, Science and Research Branch, Islamic Azad University, Tehran, Iran.
[3]Department of Chemistry, Yazd Branch, Islamic Azad University, Yazd, Iran.

Accepted 26 August 2010

One group of diseases, known as amyloidoses, which includes Alzheimer's and the transmissible spongiform encephalopathies, involves deposition of aggregated proteins in a variety of tissues. These diseases are particularly intriguing because evidence is accumulating that the formation of the highly organized amyloid aggregates is a generic property of polypeptides, and not simply a feature of the few proteins associated with recognized pathological conditions. Amyloidosis refers to a group of protein folding diseases. Various innocuous and soluble proteins in physiological conditions polymerize to insoluble amyloid fibrils in several serious diseases, including Alzheimer's disease (AD) and prion diseases. Designed for the *ab initio* quantum mechanical calculations, we used the density functional theory (DFT). In this theoretical study, we used HF and DFT (BLYP, B3LYP) method for calculation energy, chemical shift nucleus magnetic resonance and quantity thermodynamic by DFT-IR and DFT-NMR. The basis set used were STO-3G, 3-21G,6–31G,6–31G* and 6-31G. The solvation of biomolecules is essential in molecular biology, since diverse processes involve proteins interacting in changing solvent–solute systems. In conclusion, to obtain more information, we calculated thermo chemical parameters to obtain that the dielectric constant of solvents show a significant role in the Aβ1–42.**

Key words: Amyloidosis, *ab initio* quantum mechanical calculations, DFT, dielectric constant

INTRODUCTION

A living organism may contain as many as 100 000 different types of protein. Following synthesis on the ribosome, each protein molecule must fold into the specific conformational state that is encoded in its sequence in order to be able to carry out its biological function (Dobson and Fersht, 1995). In the cell, folding takes place in a complex and highly crowded environment, and the folding process is aided by a range of auxiliary proteins (Gething and Sambrook, 1992; Ellis and Hartl, 1999). The ability of proteins to fold to their functional states following synthesis in the intracellular environment is one of the most remarkable features of biology (Dobson, 2001). Amyloid, first recognized by Virchow in 1854, was a pathological starch-like proteinaceous substance, deposited between cells in various tissues and organs of the body in a wide variety of clinical settings (Xing et al., 2002). The dominant component of the core of the senile plaque is Aβ. Aβ comprises peptides of approximately 39-/43 amino acid residues derived from APP; a large 695 amino acid transmembrane molecule expressed in neurons (Ponte et al., 1988). The APP protein is cleaved by a series of enzymes during cellular metabolism. Aβ peptide is liberated by the actions of β-secretase at N-terminal site to the start of the transmembrane domain and γ-secretase at a g site within the transmembrane domain. A second alternative cleavage pathway involving α-secretase and γ-secretase results in cleavage of the APP protein in the center of the Aβ peptide region and therefore precludes the formation and deposition of Aβ peptide (Xing and Higuchi, 2002). A large body of evidence assigns a critical role in the pathogenesis of Alzheimer's disease (AD) to the amyloid-β (Aβ) peptide, a cleavage product of the amyloid precursor protein, which is predominantly 40 or 42 amino acids in length (Goedert and Spillantini, 2006; Haass and Selkoe, 2007; Hardy and Selkoe, 2002; Lansbury and

*Corresponding author. E-mail: smollaamin@gmail.com.

Lashuel, 2006). Computer simulations have been extensively carried out to understand the mechanism of protein folding processes. The most microscopic level of the computational studies of protein folding uses atomic models of a protein as well as its environment (Kim et al., 2005). Thus, many researchers have turned to computer simulations at various levels of resolutions to gain a better understanding of the molecular-level details in fibrils formation (Ma and Nussinov, 2006; Wang et al., 2008).

While the amino acid composition and structure intrinsically determine the aggregation behavior of a protein, the effects of solution properties, including temperature, pH, salt type and concentration, co-solutes, preservatives and surfactants, are also significant (Chi et al., 2003). It has been shown (Qin et al., 2007; Tanksale et al., 2002; Nguyen and Hall, 2002; Zhang et al., 1998; Speed et al., 1996; Raman et al., 1996; Georgiou et al., 1994; Broglia et al., 1998; Clark et al., 1998) both experimentally and through simulations that aggregation starts from a partially unfolded conformation with more exposed hydrophobic regions as compared to its native counterpart (Zhang et al., 2008).

So far, all calculations have been in the gas phase, while gas phase predications are appropriate for many purposes and inadequate for describing many systems in solutions. The solvent effect is taken into account via the self consistent reaction field (SCRF) method. This method is based on Onsager reaction field theory of electrostatic solvation. In this model, the solvent is considered as a uniform dielectric with a given dielectric constant (ε). The solute is placed into a cavity within the solvent. SCRF approaches differ in how they define the cavity and reaction field (Monajjemi and Chahkandi, 2005). Solvent effects on electronic structure of molecules have been investigated by many chemists and physicists to understand molecular structure, mechanism of chemical reactions in solution etc. by using quantum – chemical calculations and molecular dynamics simulations. Physical properties such as geometry of molecules and charge distribution in solution often vary from those in vacuum (Ryde et al., 2001). IR absorption spectroscopy has been applied to elucidate a protein structure by overcoming these problems experimentally and theoretically. Among the application to protein science, IR spectroscopy has recently been put to use on amyloid fibril analysis (Monajjemi et al., 2003).

We have used non empirical calculation in one of the first detailed studies of β-amyloid peptide (Aβ1–42), geometries, energies, enthalpies, Gibbs free energies, entropies, and other thermo chemical properties with special prominence of solvent effect on it. We have optimized the geometries of the (Aβ1-42) peptide in a range of solvents using the Onsager model at the HF, BLYP and B3LYP levels of theory and compared our results with those obtained for the gas phase as well; the effect of the permittivity of solvents on the steadiness of this structure was explored and discussed. The calculations were performed using the STO-3G, 3-21G, 6-31G, 6-31G*, 6-31G**, basis set.

COMPUTATIONAL DETAILS

Quantum chemical calculations were used by means of the GAUSSIAN 98 program package (Frisch et al., 1998). IR spectra studied in conjunction with normal mode calculations by quantum chemical methods provide details of conformational studies. The first step of the calculations consisted of geometry optimization of the amyloid-β molecules (Amiri et al., 2007).

The solute is placed into a cavity within the solvent. SCRF approaches differ in how they define the cavity and reaction field (Monajjemi and Chahkandi, 2005).

The equilibrium free energy of solvation can be divided into smaller contributions corresponding to cavitation; universal solvation effect such as solute-solvent electrostatic, dispersion and repulsion interactions, and no universal specific interaction, such as intermolecular hydrogen bonding or electron donor-electron acceptor interactions (Schleyer, 1998):

$$\Delta G\ (\text{solvation}) = \Delta G(\text{electrostatic}) + \Delta G(\text{dispersion}) + \Delta G(\text{repulsion}) + \Delta G(\text{cavitation}) + \Delta G\ (\text{specific}). \quad (1)$$

At first, we have modeled the 42-amino acid β-amyloid peptide (Aβ1–42) with Hyper Chem 7 package. The *ab initio* molecular calculations were carried out using the GAUSSIAN 98 program. Geometry optimization in the gas phase and solution for Aβ1–42 was performed at the HF, BLYP, B3LYP level with the STO-3G, 3-21G, 6-31G, 6-31G*, 6-31G** basis sets (Nafisi et al., 2004).

The enthalpies, free energies, entropies of (Aβ1–42) were carried out in solution and gas phase (Monajjemi and Chahkandi, 2005).

$$\Delta G = \Delta H - T\Delta S \quad (2)$$

NMR is an ideal tool for investigating the structural and dynamic differences between the native and mutant proteins. *Ab initio* calculation of nuclear magnetic shielding has become an indispensable aid in the analysis of molecular structure and accurate assignment of NMR spectra of compounds (Monajjemi et al., 2007). NMR is based on the quantum mechanical property of nuclei. The chemical shielding refers to the phenomenon, which associated with the secondary magnetic field created by the induced motions of the electrons that surrounding the nuclei when in the presence of an applied magnetic field.

For chemical shielding (CS) tensor, which describes how the size of shielding varies with molecular orientation, we recurrently use the following convention for the three principle component:

$$\sigma_{11} \leq \sigma_{22} \leq \sigma_{33} \quad (3)$$

The three values of the shielding tensor are frequently expressed as the isotropic value (σ_{iso}), anisotropy shielding ($\Delta\sigma$) and asymmetry parameter (η) (Fazaeli et al., 2003).

Calculations of nucleus-dependent and -independent chemical shifts were carried out using the gauge-invariant atomic orbital (GIAO) approach (Aghaie et al., 2008). The magnetic susceptibility was computed using continuous set gauge transformation (CSGT) methods (Nafsi et al., 2007).

The energy of solvation can be divided into terms that explain the bulk solvent and terms that specify the first solvation shell. The bulk solvent contribution is principally the result of dielectric shielding of electrostatic charge interactions. In the simplest form, it can be included in electrostatic interactions by means of the dielectric constant ε, as in the Coulomb interaction equation (Young, 2001).

$$\varepsilon = q_i q_j / \varepsilon r_{ij} \quad (4)$$

Table 1. Relative thermo chemical parameters (enthalpy ΔH Kcal/mol, and Gibbs free energy ΔG Kcal/mol, and entropy ΔS cal/ (mol K), of (Aβ1–42) obtained in gas phases.

Basis set	Method	ΔH Kcal/mol		ΔG Kcal/mol		ΔS cal/ (mol K)	
		298	302	298	302	298	302
		300	304	300	304	300	304
STO-3G	HF	-0.395326	-0.13554	0	-0.504511	0	0.864
		-0.270453	0	-0.242216	-0.768062	0.415	1.313
	BLYP	-0.320653	-0.11044	0	-0.441133	0	0.701
		-0.219625	0	-0.211468	-0.671427	0.337	1.066
	B3LYP	-0.336968	-0.116088	0	-0.471254	0	0.736
		-0.230921	0	-0.225901	-0.717234	0.354	1.118
3-21G	HF	0.442388	-0.152483	0	-0.518316	0	0.967
		-0.303083	0	-0.248491	-0.788769	0.465	1.469
	BLYP	-0.401601	-0.13805	0	-0.510786	0	0.878
		-0.275473	0	-0.244726	-0.777474	0.422	1.335
	B3LYP	-0.438623	-0.1506	0	-0.533376	0	0.959
		-0.300573	0	-0.256021	-0.812614	0.461	1.457
6-31G	HF	-0.451801	-0.15562	0	-0.536514	0	0.988
		-0.309986	0	-0.257276	-0.816379	0.475	1.501
	BLYP	-0.405366	-0.139305	0	-0.503884	0	0.886
		-0.277983	0	-0.241588	-0.766807	0.426	1.345
	B3LYP	-0.459331	-0.157503	0	-0.545299	0	1.005
		-0.315006	0	-0.261668	-0.830184	0.483	1.526
6-31G*	HF	-0.452429	-0.15562	0	-0.525846	0	0.989
		-0.309986	0	-0.252256	-0.800692	0.475	1.502
	BLYP	-0.438623	-0.151228	0	-0.532121	0	0.959
		-0.301201	0	-0.255393	-0.809477	0.461	1.457
	B3LYP	-0.505135	-0.17319	0	-0.612954	0	1.102
		-0.345126	0	-0.293555	-0.932979	0.53	1.673
6-31G**	HF	-0.452429	-0.15562	0	-0.525846	0	0.989
		-0.309986	0	-0.252256	-0.800692	0.475	1.502
	BLYP	-0.448664	-0.154365	0	-0.548436	0	0.981
		-0.307476	0	-0.262923	-0.834577	0.472	1.491
	B3LYP	-0.513296	-0.176328	0	-0.622481	0	1.123
		-0.351401	0	-0.298063	-0.947527	0.54	1.705

RESULTS AND DISCUSSION

IR data

Thermo chemical analysis is done for (Aβ1–42). The values of Δ*H*, Δ*S* and Δ*G* are reported in Tables 1 and 2 and Figures 1 and 2, in which the individual terms are referred to temperatures of 298, 300, 302 and 304 K. As can be seen, the Δ*G* values decreased with increasing of temperatures, although the relative differences of the ΔG

Table 2(a). Relative thermo chemical parameters (enthalpy ΔH kcal/mol, and Gibbs free energy ΔG kcal/mol, and entropy ΔS cal/ (mol K), of (Aβ1–42) obtained in water and other solvent using different methods (STO-3G).

Solvent	Method	ΔH kcal/mol		ΔG kcal/mol		ΔS cal/ (mol K)	
		298	302	298	302	298	302
		300	304	300	304	300	304
Water	HF	-0.259158	0	0	-0.504511	0	0.864
		-0.134913	0	-0.241588	-0.504511	0.415	0.864
	BLYP	-0.320653	-0.11044	0	-0.441133	0	0.702
		-0.220253	0	-0.211468	-0.672054	0.337	1.067
	B3LYP	-0.336341	-0.11546	0	-0.471254	0	0.736
		-0.230293	0	-0.226528	-0.717234	0.354	1.118
D M S O	HF	-0.259158	0	0	-0.504511	0	0.865
		-0.134913	0	-0.241588	-0.504511	0.416	0.865
	BLYP	-0.321281	-0.11044	0	-0.441761	0	0.701
		-0.220253	0	-0.212095	-0.672054	0.337	1.066
	B3LYP	-0.336341	-0.11546	0	-0.471254	0	0.736
		-0.230921	0	-0.226528	-0.717234	0.353	1.118
acetone	HF	-0.259158	0	0	-0.504511	0	0.865
		-0.134913	0	-0.242216	-0.504511	0.416	0.865
	BLYP	-0.321281	-0.11044	0	-0.441761	0	0.702
		-0.220253	0	-0.212095	-0.672054	0.337	1.066
	B3LYP	-0.336341	-0.11546	0	-0.471254	0	0.736
		-0.230293	0	-0.226528	-0.717234	0.354	1.119
Chloroform	HF	-0.259158	0	0	-0.504511	0	0.865
		-0.134913	0	-0.241588	-0.504511	0.416	0.865
	BLYP	-0.321281	-0.11044	0	-0.441133	0	0.701
		-0.220253	0	-0.211468	-0.671427	0.337	1.066
	B3LYP	-0.336341	-0.11546	0	-0.471254	0	0.736
		-0.230921	0	-0.226528	-0.717234	0.353	1.118

are almost the same as the Δ*H*. Therefore, in this paper, by using *ab initio* calculations and a quantum chemical approach, we analyse the Gibbs free energy of the formation of the base in gas and solution phases. The calculations of the IR frequencies and intensities were performed at the HF, BLYP, B3LYP levels with the STO-3G, 3-21G, 6-31G, 6-31G* and 6-31G** basis sets. The influence of the solvent on the relative stability of active site was studied by means of the Onsager approach.

The effect of solvents on the stabilization of Aβ1–42 show interesting results. Aβ1–42 was studied in the gas phase (ε = 1) and in various solvent media with dielectric constants of water (ε = 78.39), DMSO (ε = 46.7), Acetone (ε =20.7), Chloroform (ε = 4.9) at temperatures of 298, 300, 302 and 304 K.

We found that the Gibbs free energies (ΔG) of Aβ1–42 in solution are smaller than when in the gas phase, because interactions in solution are stronger than in the

Table 2(b). Relative thermo chemical parameters (enthalpy ΔH kcal/mol, and Gibbs free energy ΔG kcal/mol , and entropy ΔS cal/ (mol K),of (Aβ1–42) obtained in water and other solvent using different methods (3-21G).

Solvent	Method	ΔH kcal/mol		ΔG kcal/mol		ΔS cal/ (mol K)	
		298	302	298	302	298	302
		300	304	300	304	300	304
Water	HF	-0.441761	-0.151855	0	-0.518316	0	0.967
		-0.303083	0	-0.248491	-0.788769	0.465	1.469
	BLYP	-0.401601	-0.13805	0	-0.512669	0	0.878
		-0.275473	0	-0.245981	-0.779984	0.422	1.335
	B3LYP	-0.439251	-0.151228	0	-0.534631	0	0.959
		-0.301201	0	-0.256021	-0.813242	0.461	1.457
D M S O	HF	-0.442388	-0.152483	0	-0.518316	0	0.967
		-0.303711	0	-0.248491	-0.789397	0.465	1.469
	BLYP	-0.401601	-0.13805	0	-0.512669	0	0.879
		-0.275473	0	-0.245981	-0.780612	0.422	1.335
	B3LYP	-0.439251	-0.151228	0	-0.534631	0	0.96
		-0.301201	0	-0.256648	-0.813869	0.462	1.458
Acetone	HF	-0.442388	-0.151855	0	-0.518316	0	0.967
		-0.303083	0	-0.248491	-0.789397	0.465	1.469
	BLYP	-0.401601	-0.13805	0	-0.512669	0	0.878
		-0.275473	0	-0.245981	-0.780612	0.422	1.334
	B3LYP	-0.439251	-0.151228	0	-0.534004	0	0.959
		-0.301201	0	-0.256021	-0.813242	0.461	1.457
Chloroform	HF	-0.482566	-0.192033	0	-0.518944	0	0.966
		-0.343261	0	-0.249118	-0.781749	0.464	1.48
	BLYP	-0.401601	-0.13805	0	-0.512041	0	0.878
		-0.275473	0	-0.245353	-0.779357	0.422	1.334
	B3LYP	-0.439251	-0.152117	0	-0.53	0	0.966
		-0.301201	0	-0.25188	-0.808474	0.461	1.457

gas phase. The interaction energies of the Aβ1–42 decrease as the dielectric constant of solvents increases according to HF, BLYP and B3LYP calculations. The results obtained at the B3LYP/6-31G** level are more negative than those of the others calculations because these methods differently take correlation energy into account. (Figure 2b, Table 2e)

As regards the high dielectric constant of water molecules surrounding the hydrophilic part of amino acid chains, we optimized these parameters much better than for the other solvents. The best results in various solvent media were obtained at the B3LYP level of theory.

Free energy variations in terms of dielectric constant at four levels of theory and four temperatures obtained using STO-3G, 3-21G, 6-31G, 6-31G* and 6-31G** basis sets are plotted in Figure 2. We observed that the dielectric constant changes from DMSO (ε = 46.7), Acetone (ε =20.7) to polar water (ε = 78.39) Chloroform (ε = 4.9) at 298, 300, 302 and 304 K. The Gibbs free energies decrease at B3LYP levels. Table 2 and Figure 2 shows that the Gibbs free energies of interactions (Δ*G*) of Aβ1–42 in solution are more negative than in the gas

Table 2(c). Relative thermo chemical parameters (enthalpy ΔH kcal/mol, and Gibbs free energy ΔG kcal/mol, and entropy ΔS cal/ (mol K), of (Aβ1–42) obtained in water and other solvent using different methods (6–31G).

Solvent	Method	ΔH kcal/mol		ΔG kcal/mol		ΔS cal/ (mol K)	
		298	302	298	302	298	302
		300	304	300	304	300	304
Water	HF	-0.451801	-0.154993	0	-0.536514	0	0.988
		-0.309358	0	-0.257276	-0.816379	0.475	1.501
	BLYP	-0.404738	-0.139305	0	-0.504511	0	0.885
		-0.277356	0	-0.242216	-0.768062	0.425	1.345
	B3LYP	-0.459331	-0.15813	0	-0.545926	0	1.005
		-0.315006	0	-0.261668	-0.831439	0.483	1.527
D M S O	HF	-0.452429	-0.15562	0	-0.535886	0	0.988
		-0.309986	0	-0.257276	-0.816379	0.475	1.501
	BLYP	-0.405366	-0.139305	0	-0.504511	0	0.885
		-0.277983	0	-0.241588	-0.768062	0.425	1.345
	B3LYP	-0.459959	-0.15813	0	-0.545926	0	1.005
		-0.315006	0	-0.261668	-0.830812	0.483	1.526
Acetone	HF	-0.451801	-0.15562	0	-0.536514	0	0.988
		-0.309986	0	-0.257276	-0.816379	0.475	1.5
	BLYP	-0.404738	-0.139305	0	-0.504511	0	0.885
		-0.277983	0	-0.241588	-0.767434	0.425	1.345
	B3LYP	-0.387168	-0.085968	0	-0.545926	0	1.005
		-0.242843	0	-0.261668	-0.907367	0.483	1.54
Chloroform	HF	-0.451801	-0.154993	0	-0.535886	0	0.988
		-0.309358	0	-0.256648	-0.815752	0.475	1.501
	BLYP	-0.404738	-0.139305	0	-0.503884	0	0.886
		-0.277356	0	-0.241588	-0.767434	0.426	1.346
	B3LYP	-0.459331	-0.15813	0	-0.545926	0	1.005
		-0.315006	0	-0.261668	-0.830812	0.483	1.526

phase; that is, interactions in solution are stronger than in the gas phase.

NMR data

Calculations of the NMR shifts with the magnetic field perturbation method of GIAO (gauge in dependent atomic orbital) and CSGT (Continuous Set of Gauge Transformations) incorporated with the program Gaussian A7 package. The results of the calculations for the H5, O6, N7, C18, N19, H20, C36, N37 and H38 atoms in Aβ1–42 are presented in Table 3(a-e). The calculated magnetic shielding in Figure 3 (a,b) included σ_{iso} , σ_{aniso} chemical

Table 2(d). Relative thermo chemical parameters (enthalpy ΔH kcal/mol, and Gibbs free energy ΔG kcal/mol , and entropy ΔS cal/ (mol K),of (Aβ1–42) obtained in water and other solvent using different methods (6–31G*)

Solvent	Method	**ΔH** kcal/mol		**ΔG** kcal/mol		**ΔS** cal/ (mol K)	
		298	**302**	**298**	**302**	**298**	**302**
		300	**304**	**300**	**304**	**300**	**304**
Water	HF	-0.452429	-0.15562	0	-0.525846	0	0.989
		-0.310613	0	-0.252256	-0.800692	0.475	1.502
	BLYP	-0.438623	-0.1506	0	-0.533376	0	0.96
		-0.300573	0	-0.256021	-0.811987	0.461	1.458
D M S O	HF	-0.452429	-0.15562	0	-0.525846	0	0.989
		-0.310613	0	-0.252256	-0.800692	0.475	1.502
	BLYP	-0.438623	-0.1506	0	-0.532749	0	0.959
		-0.300573	0	-0.255393	-0.811359	0.461	1.458
Acetone	HF	-0.452429	-0.15562	0	-0.526474	0	0.989
		-0.309986	0	-0.252883	-0.801319	0.476	1.503
	BLYP	-0.438623	-0.1506	0	-0.532749	0	0.96
		-0.300573	0	-0.255393	-0.810732	0.462	1.458
Chloroform	HF	-0.452429	-0.15562	0	-0.526474	0	0.989
		-0.309986	0	-0.252883	-0.801319	0.475	1.502
	BLYP	-0.439251	-0.151228	0	-0.532749	0	0.959
		-0.301201	0	-0.255393	-0.810732	0.461	1.457

Table 2(e). Relative thermo chemical parameters (enthalpy ΔH kcal/mol,and Gibbs free energy ΔG kcal/mol , and entropy ΔS cal/ (mol K),of (Aβ1–42) obtained in water and other solvent using different methods (6-31G**).

Solvent	Method	**ΔH kcal/mol**		**ΔG kcal/mol**		**ΔS cal/ (mol K)**	
		298	**302**	**298**	**302**	**298**	**302**
		300	**304**	**300**	**304**	**300**	**304**
Water	HF	-0.452429	-0.15562	0	-0.525846	0	0.99
		-0.309986	0	-0.252256	-0.801319	0.476	1.503
	B3LYP	-0.513296	-0.176328	0	-0.622481	0	1.123
		-0.352028	0	-0.298691	-0.947527	0.54	1.705
D M S O	HF	-0.452429	-0.15562	0	-0.526474	0	0.989
		-0.310613	0	-0.252256	-0.801319	0.475	1.503
	B3LYP	-0.513296	-0.176328	0	-0.622481	0	1.123
		-0.352028	0	-0.298691	-0.947527	0.54	1.706
Acetone	HF	-0.452429	-0.154993	0	-0.526474	0	0.989
		-0.309986	0	-0.252883	-0.801319	0.476	1.503
	B3LYP	-0.513296	-0.176328	0	-0.622481	0	1.123

Table 2(e). Contd.

		-0.352028	0	-0.298691	-0.947527	0.54	1.706
Chloroform	HF	-0.452429	-0.15562	0	-0.525846	0	0.989
		-0.309986	0	-0.252256	-0.800692	0.475	1.502
	B3LYP	-0.513924	-0.176955	0	-0.622481	0	1.123
		-0.352028	0	-0.298691	-0.947527	0.54	1.705

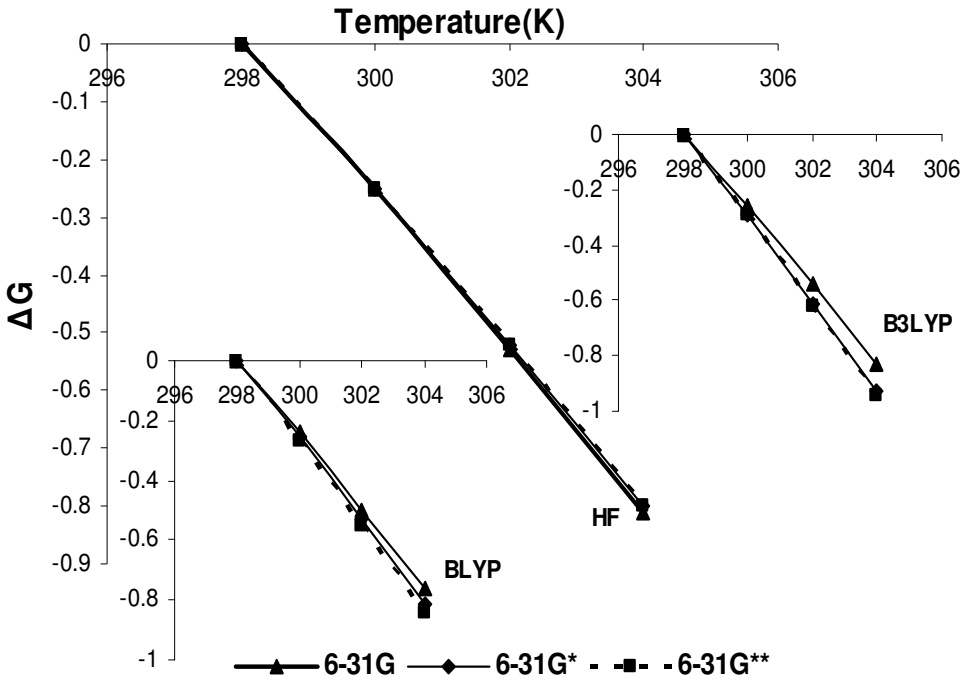

Figure 1. Comparison of Gibbs free energy ΔG (Kcal/mol) of (Aβ1–42) in gas phases obtained using the HF and DFT methods at four temperatures.

shifts was investigated by N37 absolute shielding in Aβ1–42. They are worth noting that the last approach leads to a substantial improvement in the calculated magnetic properties. Concerning the method for achievement of gauge invariance in the present case, at the B3LYP and HF levels, on the other hand, at the hybrid B3LYP level, GIAO is found to be slightly superior.

The optimized geometries were obtained from calculations at HF, BLYP, B3LYP levels with the STO-3G, 3-21G 6-31G, 6-31G*, 6-31G** basis sets. The largest σ_{iso} value of mentioned atom of Aβ1–42 was observed for H38, while the smallest one belongs to N37. As a matter of fact, the energies and thermo chemical parameters can give valuable information about structures and relative stabilities of amino acids in proteins with possible diverse mutations in humans.

Conclusion

NMR parameters are very sensitive to small changes in molecular geometry and chemical environment exhibited significant sensitivity to the intra molecular interactions. So, our obtained theoretical results emphasized on the influence of the environment factors.

This article, especially, refers to the second-order magnetic response properties (NMR), since the magnetic resonance based techniques have gained substantial value in chemistry and biochemistry in that NMR data is shown with two parameters isotropic (σiso) and anisotropic (σ_{aniso}) shielding. The calculation of nuclear magnetic resonance (NMR) parameters using *ab initio* techniques seems to be a major and a remarkable tool for investigating the variations of biological systems and provides

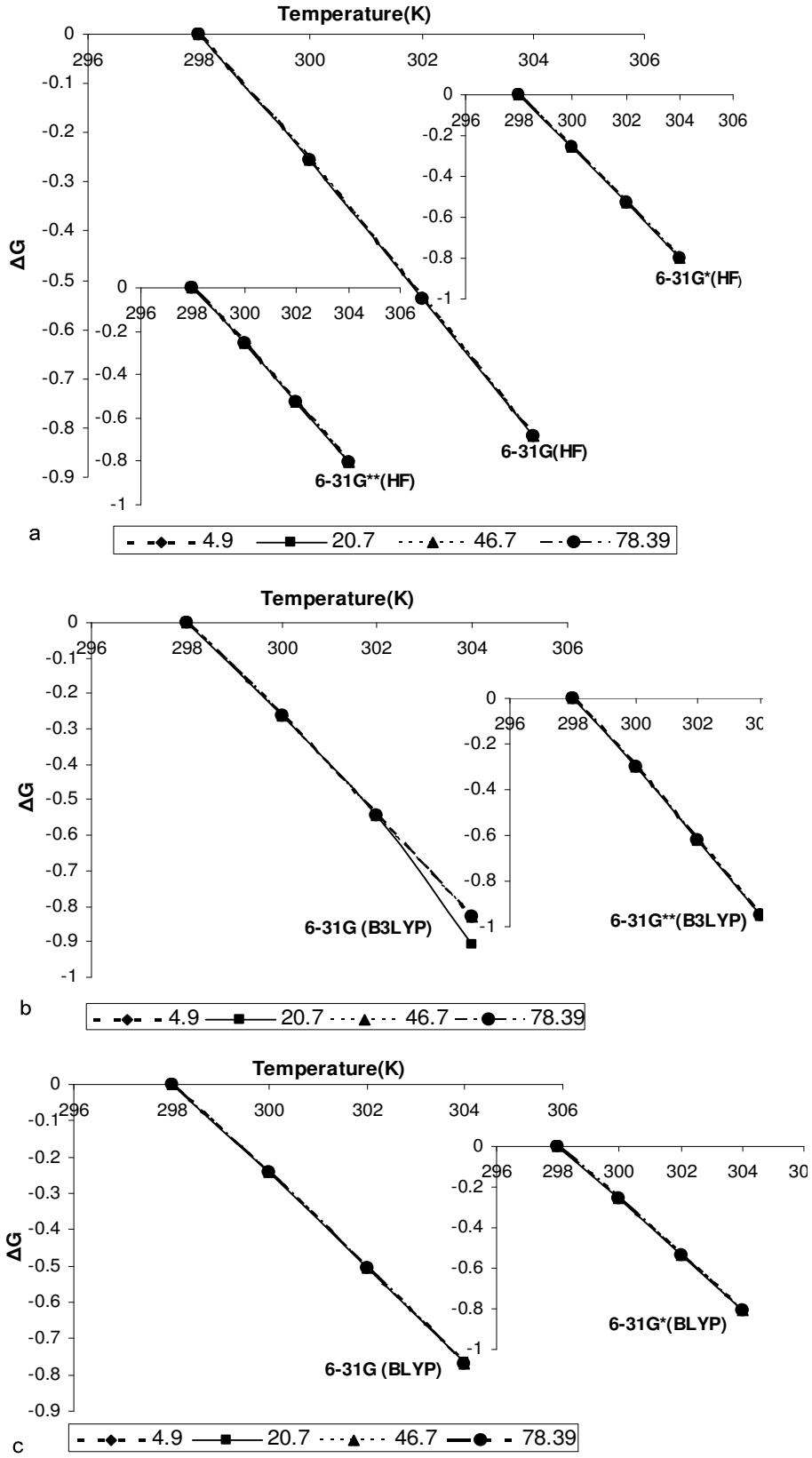

Figure 2. Comparison of Gibbs free energy ΔG (Kcal/mol) of (Aβ1–42) versus solvent media with dielectric constants of water (ε = 78.39), DMSO (ε = 46.7), Acetone (ε =20.7), Chloroform (ε = 4.9) obtained using the HF and DFT methods at four temperatures (298, 300, 302, 304K). **(a)** HF-ΔG, **(b)** B3LYP-ΔG **(c)** BLYP-ΔG.

Table 3(a). NMR parameters of (Aβ1–42) in gas phases at HF, BLYP, B3LYP levels with the STO-3G basis sets in GIAO and CSGT methods.

Basis set		STO-3G								
Method		HF								
		BLYP								
		B3LYP								
Atoms		H5	O6	N7	C18	N19	H20	C36	N37	H38
GIAO	σiso	32.1155	345.8841	279.1549	220.1305	278.4481	31.7506	220.168	-179.415	30.0652
		31.7281	294.3354	244.5639	204.0292	238.9118	30.5294	203.9623	-139.801	29.0561
		31.7431	307.1872	252.6194	207.9492	250.2774	30.7778	207.9764	-179.309	29.1317
	σaniso	15.14668	81.4767	39.9668	27.0887	32.8018	8.0773	24.9001	702.1174	9.5117
		13.7827	79.8027	33.1747	29.977	27.4827	8.3136	28.0078	596.0547	8.3832
		14.1708	79.5156	34.1512	29.3333	30.0441	8.3017	27.1879	666.9495	8.6935
	Δσ	31.98365	-9.29985	81.47675	23.33145	-17.4016	32.80175	26.6867	24.90015	-1186.71
		39.7149	-8.4236	79.80265	25.99935	-18.8396	27.4827	29.86425	28.0078	-964.341
		37.73705	-8.6639	79.51555	25.42295	-18.5191	30.0441	29.3816	27.1879	-1097.28
CSGT	σiso	30.0714	127.7645	126.6027	128.9539	126.563	31.0072	129.1046	-261.798	29.6105
		29.8985	97.1804	111.287	118.3313	106.2387	30.311	118.3646	-230.273	29.1324
		29.8761	103.894	114.1853	120.81	111.4341	30.422	120.9427	-265.48	29.0596
	σaniso	2.0523	120.9016	22.884	10.0093	24.4489	5.9905	9.2682	592.3326	6.5285
		1.9593	95.871	25.1377	12.457	35.7189	6.8394	11.9012	517.0145	7.0314
		1.9707	100.3844	25.5446	11.9479	32.2395	6.6617	11.2328	576.6498	7.0686
	Δσ	15.4538	-1.6063	120.9017	9.18185	10.0093	24.4489	10.41375	9.2682	-1069.18
		25.8573	-1.35765	-79.0098	11.60195	12.45705	35.7189	13.0411	11.9012	-869.98
		23.19145	-1.3734	-81.2862	11.1125	11.94795	32.2395	12.6939	11.23285	-995.289

Table 3(b). NMR parameters of (Aβ1–42) in gas phases at HF,BLYP,B3LYP levels with the 3-21G basis sets in GIAO and CSGT methods.

Basis set		3-21G								
Method		HF								
		BLYP								
		B3LYP								
Atoms		H5	O6	N7	C18	N19	H20	C36	N37	H38
GIAO	σiso	31.9068	280.8569	214.8438	191.2695	219.9008	29.658	191.3926	-317.535	27.9067
		31.3902	230.1825	178.9607	175.7839	174.7198	27.8568	175.9118	-237.185	26.3724
		31.4528	243.5218	187.6973	179.7952	189.8438	28.2894	180.1056	-295.417	26.694
	σaniso	12.3886	88.0392	29.38	28.7536	47.7314	7.8739	26.4602	807.2334	8.6949
		10.52	83.4777	29.1696	32.0939	44.2196	7.3636	29.8931	638.675	7.7954
		11.0256	84.917	29.0681	31.3335	46.6743	7.6033	28.7544	739.3061	8.006
	Δσ	32.4608	-7.81875	88.0391	23.6251	-20.193	47.7314	29.3636	26.46015	-1338.64
		35.97535	-6.538	83.47775	26.98125	32.09385	44.21955	33.83755	29.89315	-994.224
		35.4885	-6.87435	84.917	26.21105	-21.1428	46.6743	33.23475	28.7544	-1173.53
CSGT	σiso	28.6677	200.0196	179.321	177.1063	187.3296	27.4735	177.2728	-334.34	25.8559

Table 3(b). Contd.

	28.2842	157.5664	150.1816	162.5959	148.478	26.0706	162.677	-257.124	24.3503
	28.3319	168.3725	157.1027	166.3813	161.4418	26.3838	166.6902	-312.964	24.6469
	2.532	121.793	40.5211	18.8281	28.5343	6.4392	17.3761	764.1214	6.0944
σaniso	1.6775	118.3448	38.8306	21.7983	27.0419	6.2222	20.6085	601.8378	5.2033
	1.8337	118.8203	38.6523	21.1934	24.9637	6.3428	19.5897	698.3616	5.6355
	31.26285	-2.58345	121.793	16.71435	-15.5111	28.5342	19.75295	17.37615	-1289.1
Δσ	37.0165	-1.70605	118.3448	19.76145	21.79835	27.0419	23.3317	20.6085	-948.079
	35.94355	-1.9261	118.8203	19.1545	21.1934	24.96365	22.9738	19.5897	-1123.73

Table 3(c). NMR parameters of (Aβ1–42) in gas phases at HF,BLYP, B3LYP levels with the 6-31G basis sets in GIAO and CSGT methods.

Basis set		**6-31G**								
Method		**HF**								
		BLYP								
		B3LYP								
Atoms		**H5**	**O6**	**N7**	**C18**	**N19**	**H20**	**C36**	**N37**	**H38**
		31.704	250.7756	194.2931	183.6381	198.9847	29.523	183.7613	-369.429	27.6933
	σiso	31.2399	202.2513	157.0337	165.5325	149.3686	27.5816	165.5249	-282.318	26.0115
		31.2922	215.1664	166.1894	170.1948	166.6554	28.0448	170.4867	-346.494	26.3723
		11.8463	94.154	30.1357	29.6332	53.9127	7.6685	27.4348	846.6672	8.4155
GIAO	σaniso	9.897	93.9405	29.6726	32.805	50.5063	7.2017	31.0399	668.8258	7.3335
		10.4248	93.8841	29.6313	32.0596	52.4562	7.4274	29.6758	778.2636	7.618
		36.2101	-7.4057	94.15395	24.8606	-21.0182	53.9127	31.20315	27.4348	-1404.56
	Δσ	36.9789	-6.1303	93.94045	28.0156	32.805	50.5064	35.7655	31.0399	-1040.8
		37.24675	-6.46905	93.8841	27.2451	32.0596	52.4562	35.1591	29.67585	-1233.58
		28.5865	196.1251	165.0795	170.5278	170.6863	26.9147	170.7491	-382.256	25.1405
	σiso	28.1774	151.6884	132.3456	153.8149	126.0045	25.4319	153.856	-298.385	23.438
		28.2322	163.1826	140.245	158.1444	141.5535	25.7591	158.5162	-360.279	23.7892
		2.4584	116.8928	42.1444	27.4496	39.2243	6.318	25.8367	810.0669	6.2532
CSGT	σaniso	1.2992	117.9329	35.4905	30.8579	38.4513	6.1766	29.6826	635.1743	5.4453
		1.5806	117.1475	36.2925	30.1566	37.2191	6.2634	28.3576	741.4413	5.8643
		37.82045	-2.23335	116.8928	25.11805	27.44965	39.22425	28.90525	25.83665	-1359.15
	Δσ	41.39485	-1.31755	117.933	28.41575	30.85785	38.4513	33.2002	29.68255	-997.344
		40.92075	-1.54725	117.1475	27.73125	30.15665	37.21905	32.7284	28.3576	-1186.89

Table 3(d). NMR parameters of (Aβ1–42) in gas phases at HF,BLYP,B3LYP levels with the 6-31G* basis sets in GIAO and CSGT methods.

Basis set		**6-31G***								
Method		**HF**								
		BLYP								
		B3LYP								
Atoms		**H5**	**O6**	**N7**	**C18**	**N19**	**H20**	**C36**	**N37**	**H38**
GIAO	σiso	31.2209	255.5642	194.3455	178.0461	200.9615	28.5528	178.1672	-270.962	27.4924

Table 3(d). Contd.

		30.874	211.4736	158.6506	161.8396	153.557	26.8929	161.9728	-237.016	25.7885
		30.9001	223.4474	167.4868	166.0668	169.7768	27.2901	166.4236	-283.446	26.1762
		11.037	87.8681	30.8631	26.9909	49.455	7.3078	25.0252	701.2321	7.2889
	σaniso	9.3797	90.1772	29.8926	30.8213	46.5671	6.873	29.1057	605.6429	6.3606
		9.8478	89.3614	29.9413	29.9752	48.4461	7.0655	27.7741	687.5505	6.6502
		34.48845	-6.93145	87.86815	22.8473	-18.8494	49.455	27.9638	25.02525	-1111.17
	Δσ	36.2705	-5.8757	90.1772	26.4615	30.82135	46.5671	33.33195	29.1057	-906.157
		36.3435	-6.17155	89.36135	25.67195	-20.5189	48.44605	32.42375	27.7741	-1046.26
		28.8771	234.0455	185.9721	175.5033	194.5283	27.1817	175.7076	-277.47	26.143
	σiso	28.4441	188.3665	150.9289	160.9313	148.4828	25.6965	161.0785	-244.603	24.3544
		28.4959	200.5579	159.583	164.8222	164.1446	26.0355	165.2271	-290.299	24.7589
		6.2667	109.4368	32.2189	30.1513	41.0614	5.6618	28.3002	687.4514	5.7591
CSGT	σaniso	5.1476	111.788	31.0528	33.7303	34.9496	5.2595	32.1869	588.811	5.0844
		5.4821	110.5644	30.6882	33.0307	37.0878	5.4266	30.9713	670.872	5.4455
		40.15885	-4.06285	109.4368	27.0405	-21.4847	41.0614	30.9279	28.3001	-1095.44
	Δσ	42.26705	-3.3126	111.788	30.4306	33.73025	34.94965	35.8865	32.1869	-887.268
		42.27255	-3.52535	110.5645	29.7763	33.03075	37.0878	35.154	30.9713	-1027.64

Table 3(e). NMR parameters of (Aβ1–42) in gas phases at HF, BLYP, B3LYP levels with the 6-31G** basis sets in GIAO and CSGT methods.

Basis set		**6-31G****								
Method		**HF**								
		BLYP								
		B3LYP								
Atoms		**H5**	**O6**	**N7**	**C18**	**N19**	**H20**	**C36**	**N37**	**H38**
		30.6994	259.9412	195.8679	179.2993	202.5265	28.1599	179.4001	-274.049	27.0458
	σiso	30.4225	216.3935	160.768	163.835	155.4077	26.4117	163.9406	-237.721	25.237
		30.4407	228.2009	169.4644	167.8852	171.5861	26.8517	168.2199	-285.034	25.6738
		11.7994	83.852	30.0061	27.6061	51.3009	7.2181	25.6805	710.4958	7.6674
GIAO	σaniso	9.8224	86.1863	29.0842	31.8326	49.5158	6.8898	30.1645	611.9363	6.6168
		10.3567	85.5227	29.2255	30.8904	51.0959	7.0602	28.7256	695.0246	6.9264
	Δσ	34.6226	-7.22105	83.85205	23.3843	-19.2313	51.30085	28.54965	25.6805	-1124.99
		36.7896	-6.0393	86.1863	27.36175	31.8327	49.5158	34.37445	30.1645	-913.433
		36.77925	-6.35835	85.5227	26.48005	-21.0256	51.0959	33.3478	28.7256	-1055.85
		28.927	243.2577	189.3059	179.0942	197.5755	27.2961	179.2747	-279.724	26.1246
	σiso	28.6468	197.7229	154.4914	165.0994	151.4579	25.7665	165.2445	-244.87	24.3312
		28.664	209.883	163.0822	168.8539	167.1895	26.1373	169.2523	-291.439	24.7535
CSGT										
		8.9231	99.8791	29.8112	31.3412	44.2008	5.5711	29.3144	700.8366	6.1729
	σaniso	7.2866	102.6292	28.7767	35.425	40.7897	5.3679	33.7451	599.4613	5.2821
		7.7404	101.4971	28.5243	34.6145	42.3324	5.4952	32.4077	682.8583	5.6468

Table 3(e). Contd.

	40.1122	-5.29765	99.8791	27.92215	-22.0504	44.2008	32.04425	29.31445	-1113.75
Δσ	42.65725	-4.31755	102.6293	31.87915	35.42495	40.7897	37.6624	33.74505	-899.467
	42.5605	-4.5834	101.4971	31.09435	34.61445	42.3324	36.7729	32.40775	-1042.17

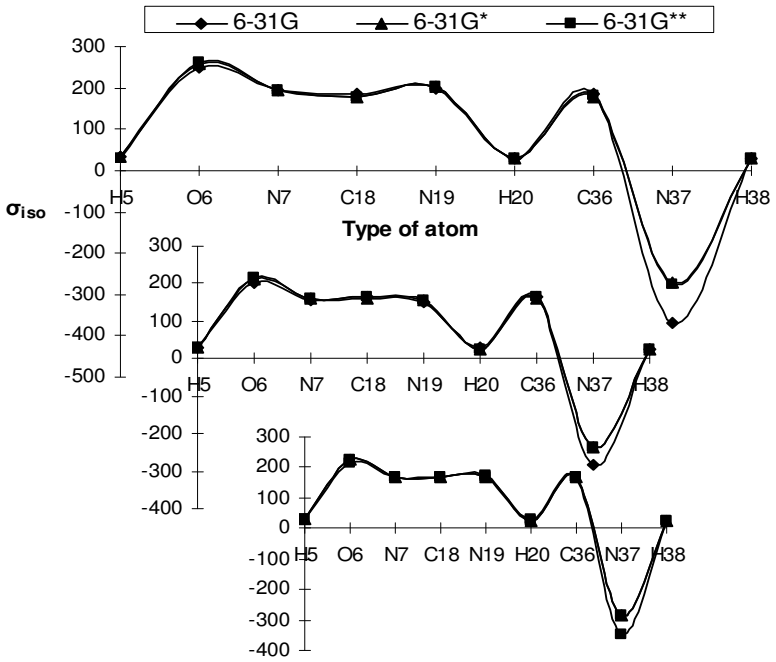

a

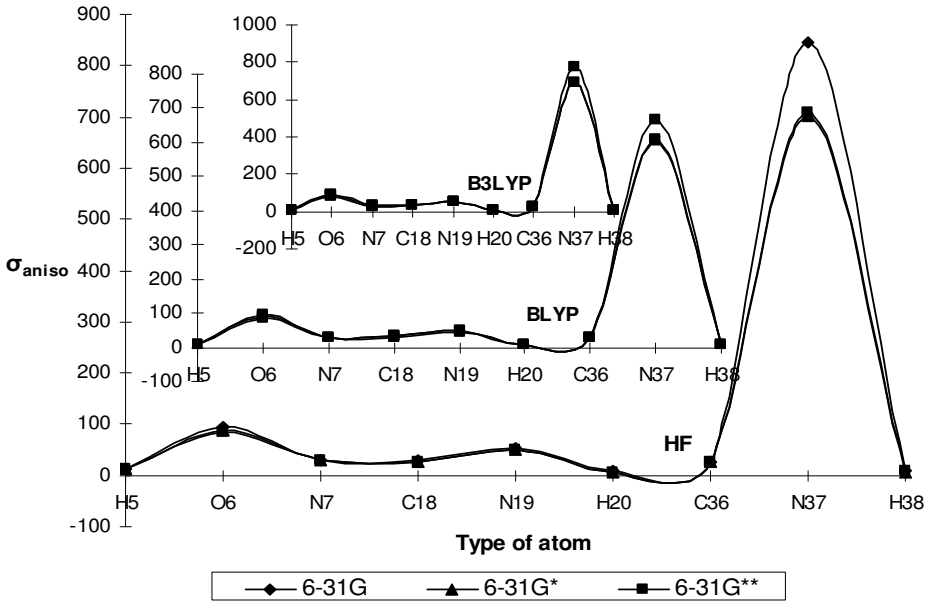

b

Figure 3. The graphs of a**)** isotropic shielding values(σ_{iso}), b**)** anisotropic shielding values(σ_{aniso}), of propose atoms of (Aβ1–42) in gas phases at the HF,BLYP,B3LYP levels with the 6-31G ,6-31G*,6-31G** basis sets in GIAO method.

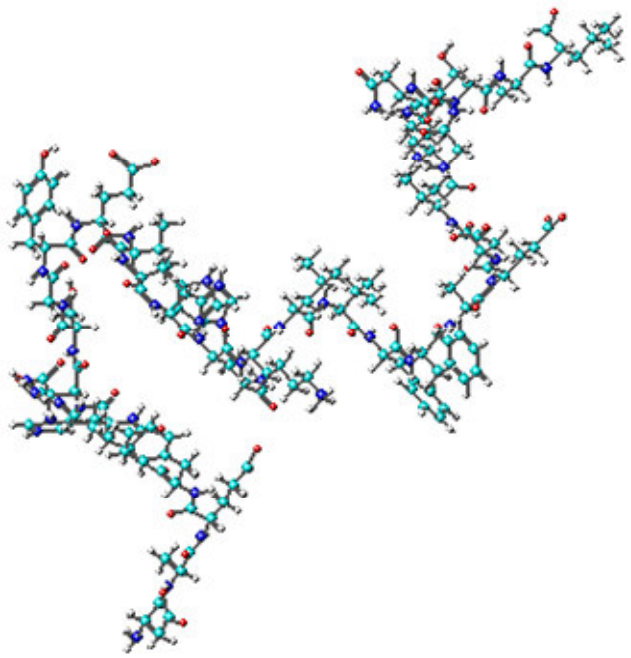

Figure 4. Optimized structure of (Aβ1–42).

information on the local environment of selected species and their nearest neighbors. Many common features were proved in the IR spectrum of Aβ1–42 (Figure 4). The consequences of the quantum-chemical modeling of the Aβ1–42 with Onsager reaction field calculations were obtained using the polarizable dielectric model. Several conclusions can be drawn. Based on our results, we explain that the free energies of interactions (Δ*G*) of Aβ1 42 in solution are more negative than in the gas phase, that is, interactions in solution are stronger than in the gas phase. Thus, the Gibbs energy of activation is lowered, and the reaction is accelerated. The present study should take measures toward complete understanding of the present system. Generally, structures and relative stabilities agree with the experiment, suggesting that studies of nanostructures can be pursued with some degree of confidence with this level of theory. The environment do not only affects the protein structure, but also protein functionality. In computational studies, it is necessary to take in to account, the modifications of solvent characteristics such as pH and ionic strength. The outcome reported in this paper indicates that it is possible to measure NMR tensors of various nuclei involving in biological compounds either in gas phase or in the presence of diverse solvent molecules theoretically. Some conclusions can be made on the basis of the observed results of the present study. Such amount of theoretical data can provide us with essential insights into the nature of molecular structures in biological systems.

In conclusion, we have shown that theoretical calculations can be used to successfully explain biochemical problems.Similar with experimental methods, they involve assumptions and interpretation, and they have their limitations, but there are many problems that are best studied using theory. Consequently, theoretical methods have become a competitive alternative to experiments for biochemical investigations.

REFERENCES

Aghaie H, Gholami MR, Monajjemi M, Ganji MD (2008).Electron transport phenomenon simulation through the carborane nano-molecular wire. J. Phys. E 40: 2965-2972.

Amiri A, Monajjemi M, Ketabi S (2007). Vibrational analysis of calix[4]arene conformers. J. Phys. Chem. Liquids. 46(4): 379-389.

Broglia RA, Tiana G, Pasquali S, Roman HE, Vigezzi E (1998) .Folding and aggregation of designed proteins. Proc. Natl. Acad. Sci. U. S. A 95: 12930-12933.

Chi EY, Krishnan S, Randolph TW, Carpenter JF (2003). Physical stability of proteins in aqueous solution: mechanism and driving forces in nonnative protein aggregation, Pharm. Res., 20: 1325-1336.

Clark ED, Hevehan D, Szela S, Maachupalli-Reddy J (1998).Oxidative renaturation of hen egg-white lysozyme. Foldingvs aggregation. Biotechnol. Prog., 14: 47-54.

Dobson CM (2001).Protein folding and human disease. Phil.Trans. R. Soc. Lond. B. 356: 133-145.

Dobson CM, Fersht AR (eds) (1995). Protein folding. Phil.Trans. R. Soc. Lond. B., 348: 1-119.

Ellis RJ, Hartl FU (1999). Principles of protein folding in the cellular environment. Curr. Opin. Struct. Biol. 9: 102-110.

Fazaeli R, Monajjemi M, Ataherian F, Zare K (2003).DFT study of metal-tetrahydroborato ligand interactionsin [Ti (CO) 4(BH4)] 2 J. Mol. Struct. (THEOCHEM).581: 51-58.

Frisch MJ, Trucks GW, Schlegel HB, Scuseria GE, Robb MA, Cheeseman JR, Zakrzewski VG, Montgomery JA, Stratmann RE, Burant JC, Dapprich S, Millam JM, Daniels AD, Kudin KN, Strain MC, Farkas O, Tomasi J, Barone V, Cossi M, Cammi R, Mennucci B, Pomelli C, Adamo C, Clifford S, Ochterski J, Petersson GA, Ayala PY, Cui Q, Morokuma K, Malick DK, Rabuck AD, Raghavachari K, Foresman JB, Cioslowski J, Ortiz JV, Stefanov BB, Liu G, Liashenko A, Piskorz Komaromi PI, Gomperts R, Martin RL, Fox DJ, Keith T, Al-Laham MA, Peng CY, Nanayakkara A, Gonzalez C, Challacombe M, Gill PMW, Johnson B, Chen W, Wong MW, Andres JL, Gonzalez C, Head-Gordon M, Replogle ES, Pople JA (1998). GAUSSIAN 98, Revision A.6, Gaussian, Inc., Pittsburgh PA .

Georgiou G, Valax P, Ostermeier M, Horowitz PM (1994). Folding and aggregation of tem beta-lactamase-analogies with the formation of inclusion-bodies in Escherichia coli. Protein Sci., 3: 1953-1960.

Gething MJ, Sambrook J (1992).Protein folding in the cell.Nature. 355: 33-45.

Goedert M, Spillantini MG (2006). A century of Alzheimer's disease. Science. 314: 777-781.

Haass C, Selkoe DJ (2007). Soluble protein oligomers in neurodegeneration: lessons from the Alzheimer's amyloid ?-peptide. Nat. Rev. Mol. Cell Biol., 8: 101-112.

Hardy J, Selkoe DJ (2002). The amyloid hypothesis of Alzheimer's disease: progress and problems on the road to therapeutics. Science. 297: 353-356.

Kim SY, Song MK, Lee J (2005) .Biophysical Chemistry Folding simulations of small proteins. 115: 195-200

Lansbury PT, Lashuel HA (2006). A century-old debate on protein aggregation and neurodegeneration enters the clinic. Nature. 443: 774-779.

Ma BY, Nussinov R (2006). Simulations as analytical tools to understand protein aggregation and predict amyloid conformation. Curr. Opin. Chem. Biol., 10: 445-452.

Monajjemi M, Aghabozorg H, Aghabozorg H (2003).Theoretical studies of rotational barriers of dithiocarbamate ligands in the square planar complexes TM (L) (L0) (H2dtc) (TM ¼ Ir, Rh). J. Molecular Structure (Theochem). 636: 49-56.

Monajjemi M, Chahkandi B (2005). Theoretical investigation of hydrogen bonding in Watson-Crick, Hoogestein and their reversed and

other models: comparison and analysis for configurations of adenine-thymine base pairs in 9 models. J. Molecular Structure: THEOCHEM 714: 43-60.
Monajjemi M, Heshmat M, Aghaei H, Ahmadia R, Zare K (2007). Bull. Chem. Soc. Ethiop., 21: 111-116.
Nafisi Sh, Monajemi M, Ebrahimi S (2004). The effects of mono- and divalent metal cations on the solution structure of caffeine and theophylline. J. Mol. Struct., 705: 35-39.
Nafsi Sh, Mohajerani N, Hadjiakhoondi A, Monajemi M, Garib F (2007). Interaction of Tl13 with mononucleotides: metal ion binding and Sugar conformation. J. Mol. Struct., 562: 35-43.
Nguyen HD, Hall CK (2002). Effect of rate of chemical or thermal renaturation on refolding and aggregation of a simple lattice protein. Biotechnol. Bioeng., 80: 823-834.
Ponte P, Gonzalez DP, Schilling J, Miller J, Hsu D, Greenberg B, Davis K, Wallace W, Lieberburg I, Fuller F (1988). A new A4 amyloid mRNA contains a domain homologous to serine proteinase inhibitors. Nature 331: 525-527.
Qin ZJ, Hu DM, Zhu M, Fink AL (2007). Structural characterization of the partially folded intermediates of an immunoglobulin light chain leading to amyloid fibrillation and amorphous aggregation. Biochemistry-Us 46: 3521-3531.
Raman B, Ramakrishna T, Rao CM (1996). Refolding of denatured and denatured /reduced lysozyme at high concentrations. J. Biol. Chem., 271: 17067-17072.
Ryde U, Olsson M, Pierloot K, Eriksson L.A (2001). editor, Elsevier, Amsterdam. Theor. Comput. Chem., 9: 1-56.
Schleyer PVR (1998). Encyclopedia of Computational Chemistry .Wiley. Chichester. 4: 2547-2574.
Speed MA, Wang DI, King J (1996). Specific aggregation of partially folded polypeptide chains: the molecular basis of inclusion body composition, Nat. Biotechnol., 14: 1283-1287.
Tanksale A, Ghatge M, Deshpande V (2002). Alpha-crystallin binds to the Aggregation-prone molten-globule state of alkaline protease: implications for preventing irreversible thermal denaturation. Protein Sci., 11: 1720-1728.
Wang J, Tan C, Chen HF, Luo R (2008).All-Atom Computer Simulations of Amyloid Fibrils Disaggregation.J. Biophysical., 95: 5037-5047.
Xing Y, Higuchi K (2002). Amyloid fibril proteins. J. Mechanisms of Ageing and Development 123: 1625-/1636.
Young DC (2001). Solvation Computational Chemistry: A Practical Guide for Applying Techniques to Real-World Problems. Wiley. New York.
Zhang L, Lu D, Liu Z (2008). How native proteins aggregate in solution: A dynamic Monte Carlo simulation. Biophys. Chem., 133: 71-80.
Zhang YL, Pan XM, Zhou JM (1998). Surface hydrophobicity and thermal aggregation of adenylate kinase, Biochem. Mol. Biol. Int., 44: 949-960.